Terahertz emission from GaAs and InAs in a magnetic field

J. N. Heyman,* P. Neocleous, and D. Hebert
Department of Physics and Astronomy, Macalester College, St. Paul, Minnesota 55105

P. A. Crowell
Department of Physics, University of Minnesota, Minneapolis, Minnesota 55455

T. Müller and K. Unterrainer
Institute for Solid State Electronics, Technical University Vienna, A-1040 Vienna, Austria
(Received 22 February 2001; published 7 August 2001)

We have studied terahertz (THz) emission from InAs and GaAs in a magnetic field, and find that the emitted radiation is produced by coupled cyclotron-plasma charge oscillations. Ultrashort pulses of THz radiation were produced at semiconductor surfaces by photoexcitation with a femtosecond Ti-sapphire laser. We recorded the integrated THz power and the THz emission spectrum as a function of magnetic field at fields up to 5.5 T, and as function of temperature for $T=10-280$ K. The maximum observed THz power is $\sim 1.6\times 10^{-13}$ J/pulse (12 μW average power) from n-InAs (1.8×10^{16} cm^{-3}) at $B=3.2$ T. We compare our results to semiclassical models of magnetoplasma oscillations of bulk free carriers and damped motion of free carriers in a two-dimensional electron gas. The bulk model describes THz emission from n-GaAs at all magnetic fields, and InAs at $B=0$. It fails to describe THz emission from InAs at nonzero magnetic fields. We show that a model including both bulk plasma oscillations and THz emission from a surface accumulation layer describes THz emission from InAs in a moderate magnetic field, but this model does not completely describe emission at fields $|B|>1.0$ T.

DOI: 10.1103/PhysRevB.64.085202 PACS number(s): 78.47.+p, 71.45.Gm, 73.20.Mf, 42.65.Re

I. INTRODUCTION

Ultrafast pulsed terahertz (THz) sources are a unique tool for time-resolved spectroscopy in condensed matter systems. The most widely used techniques for generating THz pulses are optical rectification[1] and generation of transient photocurrents at semiconductor surfaces. In the latter mechanism, photocurrents parallel to the surface can be generated between biased metallic contacts, as in an Auston switch.[2,3] Perpendicular photocurrents are generated at bare semiconductor surfaces, e.g., as photogenerated carriers accelerate in the surface depletion field.[4] Although requiring no fabrication, bare semiconductor surfaces are typically less efficient because the direction of the transient photocurrent is nearly parallel to that of the outgoing THz beam. However this limitation can be overcome by using a magnetic field to change the direction of the transient current.[5]

Recently, Sarakura *et al.*[6] have reported a substantial enhancement of the efficiency of THz generation at bare InAs surfaces by a moderate magnetic field. They claimed average emitted THz powers of ~0.7 mW using a 1 W average power Ti-sapphire pump laser. This value, which has been challenged, would make InAs the most efficient THz emitter to date. McLaughlin *et al.*[7] have examined n-InAs in magnetic fields up 8 T and obtain average emitted THz powers of ~8 μW using a 1 W average power Ti-sapphire pump. Ohatake *et al.* have investigated the THz emission from InAs for a wide variety of magnetic field geometries.[8] Weiss *et al.* have investigated THz generation from InAs and a number of other semiconductors.[9] They separate the component of the power due to enhancement by the magnetic field, and show that this component varies as the square of the field for fields $B<1$ T. However, until now there has been no detailed description of the enhancement mechanism. In addition, there is no consensus about the absolute efficiency of the generation process in InAs. Some and Nurmikko have studied coherent THz emission from undoped GaAs epilayers and modulation doped parabolic wells in a magnetic field at low temperature.[10]

In this work we present measurements of photoinduced THz emission from InAs and GaAs as a function of magnetic field. We propose a semiclassical model to describe THz generation from semiconductor surfaces in a magnetic field which includes self-consistent fields (plasma oscillations). Our work provides a simple physical picture of the emission process. We find that THz emission from n-GaAs in a magnetic field can be described as coupled plasma and cyclotron oscillations. THz emission in n-InAs at low magnetic fields can be described by including a surface plasma oscillation. At high magnetic fields, this model correctly predicts the peak frequencies of emission in InAs, but does not correctly predict the dependence of the emitted power on magnetic field.

II. EXPERIMENT

Optically pumped THz emission was measured from bulk GaAs and InAs samples in a magnetic field (see Table I). For most measurements, the samples were mounted in a horizontal split-coil superconducting magnet with a variable temperature insert (4–300 K). The sample surface was parallel or at 45° to the magnetic field. Optical excitation was provided by a mode-locked Ti-sapphire laser oscillator. The pulsewidth was 140 fs, the center wavelength was λ

TABLE I. Room-temperature carrier concentration and mobility of samples used in these measurements. Integrated THz power measured at 280 K is given for $B=0$ and the field where power is maximum (B_{max}). The excitation intensity was ~ 5 W/cm^2.

	n (10^{16} cm^{-3})	μ (cm^2/V sec)	THz power ($B=0$)	THz power ($B=B_{max}$)	$P_{10\,K}/P_{280\,K}$ ($B=0$)	$P_{10\,K}/P_{280\,K}$ ($B=B_{max}$)
n-GaAs:Si	2.4	4600	0.21	2	0.3	
n-InAs (un)	1.8	25 000	1.00	74	1.4	2.2
n-InAs:S	7.5	20 000	0.06	36	1.1	1.8
p-InAs:Zn	$\approx$20	$\approx$275	0.36	32	1.1	2.3

$=800$ nm, and the pulse repetition rate was 76 MHz. The laser was split into pump and probe beams, and the pump laser intensity at the sample surface was ≈ 5 W/cm^2 (60 nJ/cm^2/pulse). The pump beam was incident at right angles to the B field, and at 45° to the sample surface. The THz beam was emitted along the direction of the reflected pump beam. Measurements of the total emitted THz power were made with a 4.2 K Si bolometer. The bolometer was calibrated *in situ* with a black-body source. Spectroscopic measurements were made using electro-optic detection. In this technique,[11] the THz beam is mixed with a circularly polarized probe beam in a 1.0 mm thick ZnTe crystal. The THz electric field induces birefringence in the ZnTe through the second-order electro-optic effect. The change in the probe beam polarization is measured with a polarization bridge, yielding a signal proportional to the THz electric field. The THz field as a function of time following excitation is measured by varying the delay between the pump and probe pulses, and the THz spectrum (amplitude and phase) is obtained by a Fourier transformation. The pump laser was modulated with a mechanical chopper at 2.75 kHz and the signal was measured with a lock-in amplifier. The THz beam path was purged with dry N_2 gas to suppress absorption of the THz radiation by water vapor. We have also measured emission spectra by performing THz autocorrelation measurements with the bolometer. The autocorrelation spectra are generally consistent with the data presented below, but do not give phase information.

THz data acquired with the 140 fs pump laser showed little emission at frequencies above 2.5 THz, due to the finite excitation pulse width. For this reason, additional measurements were performed using a 12 fs Ti-sapphire laser oscillator. For these measurements, samples were held at room temperature in air, and a permanent magnet allowed emission to be recorded in magnetic fields of ± 0.5 T. Spectral measurements were made by THz autocorrelation, and the detector was a 4.2 K Si bolometer.

THz emission measurements were performed on n-GaAs, nominally undoped InAs and on n-type and p-type InAs. The emission was recorded as a function of temperature between 280 and 10 K. In InAs we observed a moderate increase in emitted power at low temperatures. The power fell with temperature in n-GaAs (see Table I). We observed no strong temperature dependence of the shape of the emission spectra.

The THz power versus frequency from nominally undoped n-InAs (1.8×10^{16} cm^{-3}) generated with a 12 fs pulsewidth pump laser is shown in Fig. 1(a). The $B=0$ emission spectra is dominated by a single broad peak at 1.84 THz [full width at half maximum (FWHM) $=1.0$ THz]. All InAs samples also show a sharp emission feature at 7.32 THz near the LO phonon frequency. The zero-field THz emission spectrum of n-GaAs measured with the 12 fs pump laser is shown in Fig. 1(b). The response consists of a single broad peak centered at 1.3 THz (FWHM $=1.0$ THz) and a sharp feature at 8.83 THz, near the GaAs LO-phonon frequency.

Figure 2 shows measurements of the total emitted THz power for magnetic fields parallel to the sample surface. For GaAs the response is not symmetric about $B=0$. Rather, the minimum response is at $B=0.9$ T. The emission reaches a maximum at $B=-4.5$ T, but does not reach a similar maximum at any positive field within the measurement range. In the nominally undoped InAs sample, the emission power increases by a factor of 74 between $B=0$ and 1.8 T. The power falls to a minimum at 3.8 T and then increases with field. The emitted power versus field depends weakly on the excitation intensity at low powers, and strongly on the sample doping. Emission from the more heavily doped n-type and p-type samples is much weaker than from the nominally undoped sample at zero field but is comparable at high magnetic fields (see Table I). The emission from these show maxima near

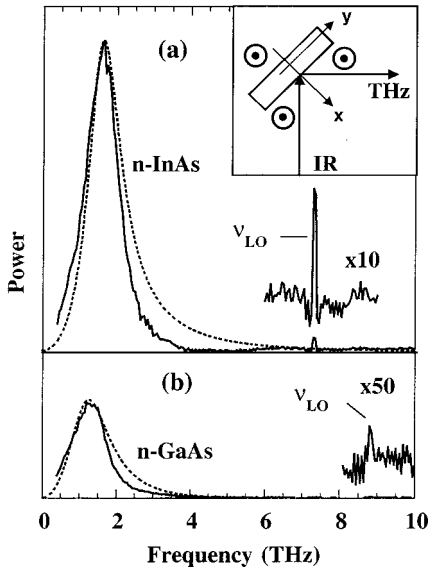

FIG. 1. (a) THz emission spectrum of n-InAs ($n=1.8\times 10^{16}$ cm^{-3}) and (b) n-GaAs ($n=2.4\times 10^{16}$ cm^{-3}) at zero magnetic field, optically excited with a 12 fs Ti:S laser oscillator. Solid lines are experimental data, dashed lines are fits to our model. The inset shows experimental geometry (B-field $\parallel$ to surface).

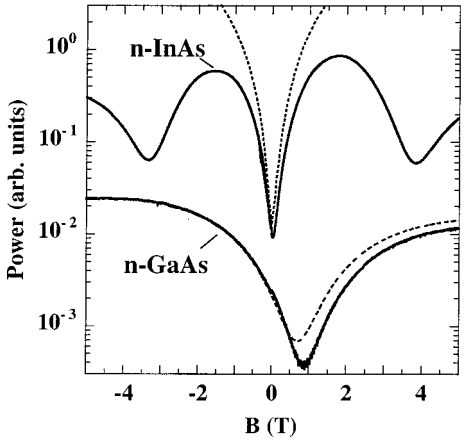

FIG. 2. Integrated THz emission from the same n-InAs and n-GaAs samples as a function of magnetic field parallel to surface. Average excitation intensity 5 W/cm^2. Solid lines are experimental data, dashed lines are fits to our model.

$B=3$ T, and then decrease without reaching a second within the measurement range. The curves are not symmetric, but unlike GaAs, all InAs samples measured show a minimum near zero field ($|B|<0.1$ T).

Calibrated power measurements of the integrated THz emission versus magnetic field were performed with the magnetic field at 45° to the sample surface. This was done because the optical throughput of our cryostat is higher in this geometry ($f/2.6$) than for magnetic fields parallel to the surface. For room-temperature InAs, a maximum average power of 12 μW was measured at $B=3.2$ T. For GaAs, the average THz power was 0.38 μW at $B=5.0$ T. The pump laser power was 10 nJ/pulse (0.8 W average power).

The THz electric field amplitude and phase versus frequency from n-GaAs and InAs excited with a 140 fs pump were obtained for magnetic fields from $B=+5$ to -5 T. The n-GaAs spectra are shown in Fig. 3(a). The sample temperature was $T=280$ K. At $B=0$, the response consists of a single broad peak. At positive magnetic fields the peak splits into two broad features which are distinct up to $B=1.5$ T. For negative fields in this same range, the two features are not distinct. Overall, the center frequency of the response shifts to lower frequencies at high fields. Figure 3(b) shows the phase of the signal at 1.1 THz, the maximum of the zero-field spectrum. A phase shift of π radians is observed between $B=+0.5$ and $+1.0$ T.

Figures 4 and 5 show the magnetic field dependence of the emission spectra from nominally undoped n-InAs (1.8×10^{16} cm^{-3}). The broad feature observed at $B=0$ evolves and moves to lower frequency with increasing field. However, the emission becomes dominated by a distinct low-frequency feature which peaks near $\upsilon\approx0.35$ THz. The phase of this low frequency component shifts by π radians at $B=0$, while the phase at $\upsilon=1.84$ THz changes at $B=+0.2$ T. Emission spectra of the more heavily doped samples are dominated by a similar low-frequency component at nonzero magnetic fields, and the phase of this component also shifts by by π radians at $B=0$. Spectra were also measured with the magnetic field at 45° to the surface (Fig. 6).

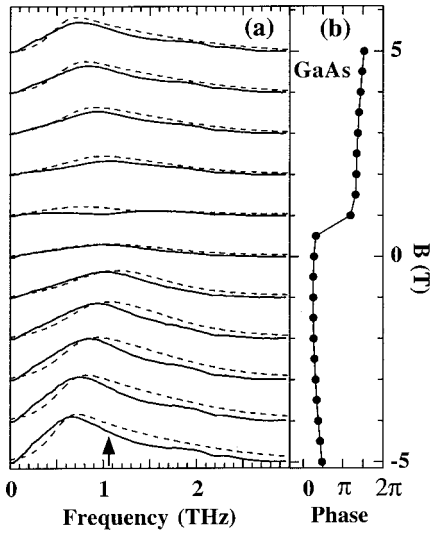

FIG. 3. (a) n-GaAs: THz electric field amplitude versus frequency as a function of magnetic field from $B=-5-+5$ T at 1 T intervals. Curves offset for clarity. Dashed lines are calculated from bulk magneto-plasma model. (b) Phase versus magnetic field at the frequency of the peak of the $B=0$ spectrum (indicated by arrow).

III. DISCUSSION

A. Model

THz emission from n-GaAs surfaces at zero magnetic field has been described by Kersting *et al.*[12,13] In their model, photoexcited carriers screen the surface depletion field.

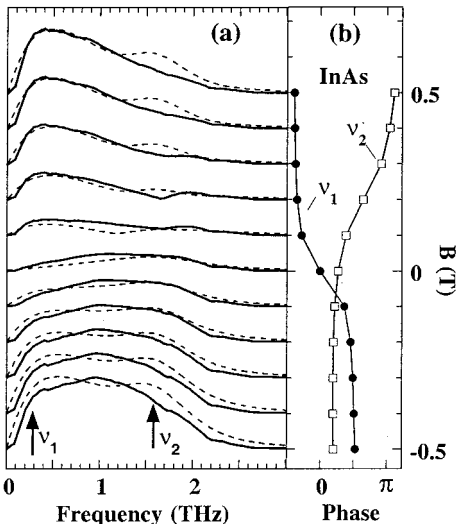

FIG. 4. (a) n-InAs: THz electric field amplitude versus frequency as a function of magnetic field at 0.1 T intervals from $B=-0.5-+0.5$ T. Curves offset for clarity. Dashed lines are from model carriers in the bulk and surface accumulation layers. (b) Phase versus magnetic field at $\nu_1=360$ GHz and at the $B=0$ plasma frequency ($\nu_2=1.8$ THz). Note phase of signal at ν_1 shifts by π radians at $B=0$.

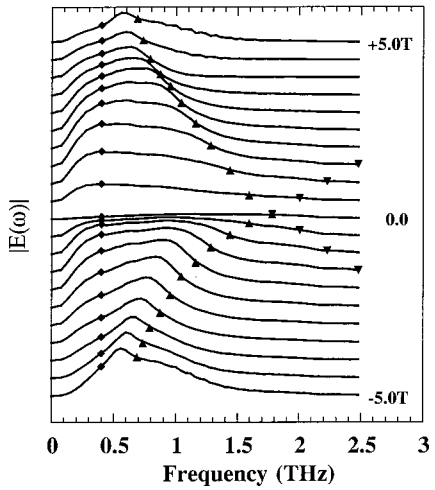

FIG. 5. *n*-InAs: THz electric field amplitude versus frequency as a function of magnetic field from $B=-5-+5$ T at 0.5 T intervals. Curves offset for clarity. Markers show calculated upper and lower branch magnetoplasma frequencies calculated for zero damping, and predicted frequency of peak emission from surface layer.

This transient change excites plasma oscillations in the bulk electron gas which are the dominant source of THz radiation in *n*-type samples. Since these are low-energy excitations of a cold electron gas, the process can be treated adequately by a semiclassical model. It is straightforward to extend this treatment to include a magnetic field. We will show that the resulting model describes THz emission from *n*-GaAs surfaces in a magnetic field. In contrast, a more detailed model[14] which treats carrier scattering on a microscopic level, but ignores self-consistent electric fields does not fit our data.

We expect that this bulk magneto-plasma model is too simple to describe InAs. Hot carrier effects may play an important role: radiation from our Ti:S laser ($h\nu=1.55$ eV)

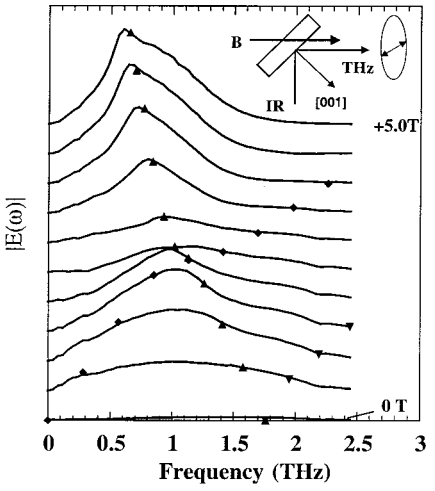

FIG. 6. *n*-InAs: Amplitude of the transverse component of the THz electric field versus frequency as a function of magnetic field 45° to surface, from $B=0-5$ T at 0.5 T intervals. Curves offset for clarity. Markers show magnetoplasma frequencies and cyclotron frequency of surface layer electrons calculated for zero damping. Inset: experimental geometry of this measurement.

can excite electrons from the heavy, light and split-off hole bands to the Γ valley of this narrow-gap semiconductor ($E_g=0.35$ eV), although other conduction-band minima are not accessible. In addition, the Fermi-level is pinned in the conduction band at the InAs surface, and magnetotransport[15] and photoelectron[16] spectroscopy have identified a surface accumulation layer in InAs with typical carrier densities of order $10^{12}\,\mathrm{cm}^{-2}$. This produces two difficulties for the bulk plasma model. First, the number of free-carriers in the surface layer is comparable to or larger than the number in the bulk photoexcited region, suggesting that the surface carriers may play an important role in THz emission. In addition, there is no surface depletion field to provide initial excitation of the electrons.

We have constructed two semiclassical models to describe our measurements. The first describes a homogeneous three-dimensional (3D) plasma of electrons in an electric and magnetic field. The second model is designed to treat electrons in the surface accumulation layer of InAs. It consists of an electron plasma confined in one dimension by a strong harmonic potential. Since we are primarily interested in describing the emission of electromagnetic radiation in these models, we examine the motion of charge in the long-wavelength limit ($q=0$). In order to obtain simple, tractable models, we have neglected hot carrier effects. In addition, we do not treat the initial excitation in detail. Instead, we assume an impulsive excitation and calculate the response of the system.

The dynamics of a homogeneous 3D plasma of charge are well understood. Displacement of charge in a conductor in crossed magnetic field and electric fields ($\mathbf{B}\|\hat{\mathbf{z}}$ and $\mathbf{E}\|\hat{\mathbf{x}}$) generally produces oscillatory motion. It can be shown that the effect of the electric field is simply to shift the origin of the electron oscillations, and the problem will now be considered in the shifted coordinate system to eliminate **E**. The displacement and velocity of the charge perpendicular to the *B* field is determined by the equation

$$\mathbf{a}=-\omega_p^2\mathbf{r}-\frac{e\mathbf{v}\times\mathbf{B}}{m^*}-\gamma\mathbf{v}, \tag{1}$$

where ω_p is the classical plasma frequency. The damping parameter γ is an effective scattering rate, which in Drude theory is related to the mobility. For the case of the initial displacement and velocity perpendicular to **B** the eigenvalues for a single-component plasma of electrons are

$$\omega_\pm=\tfrac{1}{2}[(\omega_c+i\gamma)\pm\sqrt{(\omega_c+i\gamma)^2+4\omega_p^2}], \tag{2}$$

where ω_c is the cyclotron frequency and the normal modes of the system describe clockwise and counterclockwise circular motion in the *xy* plane. This can be easily understood: For $B=0$, the in-plane equations of motion are identical to those of a 2D harmonic oscillator. The two degenerate, independent solutions describe clockwise and counterclockwise circular motion. A magnetic field perpendicular to the plane lifts the degeneracy. This model can be extended to include light and heavy holes as well. The equations of motion then include the interaction between each charged species. However, our simulations predict that the THz emission is dominated by the motion of electrons.

The THz emission from the oscillating plasma is calculated in the electric dipole approximation

$$E_{\mathrm{rad}}(t)=\frac{\mu_0}{4\pi}\left(\frac{\sin(\theta)}{r}\right)\ddot{P}(t-r/c), \tag{3}$$

where $\mathbf{P}$ is the net dipole moment, and θ is the angle between $\ddot{\mathbf{P}}$ and the direction of the emitted THz beam inside the sample.

To model THz emission from InAs, we include bulk plasma oscillations and a two-dimensional plasma confined at the sample surface. To treat this surface charge layer we introduce a strong harmonic confinement potential which restricts motion perpendicular to the surface. In addition, in the long-wavelength limit, there is no space-charge field induced by motion parallel to the surface. The equation of motion is then

$$\mathbf{a}=-\omega_s^2\mathbf{x}-\frac{e\mathbf{v}\times\mathbf{B}}{m^*}-\gamma\mathbf{v}, \tag{4}$$

where ω_s is the intersubband plasma frequency in the parabolic surface-confined layer. For a carrier density of $n_s \approx 10^{12}\,\mathrm{cm}^{-2}$ we expect $\omega_s \sim 15\,\mathrm{THz}$, which is outside of the spectral region investigated. Ignoring damping, the response of this system consists of a high-frequency mode at $\omega_+ = \sqrt{\omega_s^2+\omega_c^2}$ and a low-frequency mode at $\omega_- = 0$.

Comparison with experiment requires that we use physically reasonable initial conditions. We set the initial displacement and the initial velocity of all the carriers to zero. In the shifted coordinate system, the initial displacement of the electrons is then perpendicular to the surface. We account for the finite duration of excitation by convoluting the response function with a Gaussian whose width τ represents the duration of the excitation of the system. The lower limit on this time is the laser pulse width (140 fs), although we find we must use substantially longer times ($\tau_{\mathrm{pulse}}=350\,\mathrm{fs}$) to fit the experimental data.

For the 2D plasma these initial conditions produce an interesting result. For $B=0$, only the intersubband plasma oscillation is excited, and this produces almost no radiation in the spectral window set by our excitation pulse length. However, a magnetic field *parallel* to the surface couples the excitation into the $\omega_-=0$ mode. Charges in this mode do not oscillate, but do emit low-frequency radiation as they decelerate due to damping. This emission peaks at low frequencies: it is cut off at high frequencies $\omega/\gamma>1$, $\omega\tau_{\mathrm{pulse}}>1$ and it also is cut off at very low frequencies as $E(\omega)\propto\omega^2$ for electric dipole radiation. Unlike emission from a bulk plasma, the phase of the radiation emitted by this mechanism should change by π at $B=0$. As a result, a surface accumulation layer will contribute very weakly to the THz emission at zero magnetic field. At nonzero field we expect to observe low-frequency emission due to damped in-plane motion. In addition, a field *perpendicular* to the surface produces cyclotron motion of the carriers in the surface layer. For a field at 45° to the surface, this cyclotron motion will be driven by the initial excitation, and will also produce THz radiation.

TABLE II. Parameters used in our model calculations.

	$\gamma\ (\mathrm{sec}^{-1})$	m^*/m_0	$\gamma_s\ (\mathrm{sec}^{-1})$	ν_{12} (THz)
n-GaAs:Si	9×10^{12}	0.067		
n-InAs (un)	7×10^{12}	0.035	2×10^{12}	12

B. Comparison with experiment

The above model predicts that bulk plasma oscillations will dominate the emission at zero field. The parameters of the model include the carrier density n, the bulk damping rate γ, the effective mass m^*, and the initial displacement of the electrons. Our calculation used the measured carrier densities, while the other parameters were adjustable. As shown in Fig. 1, we can get an excellent fit to the data using the plasma model. The parameter values used to fit the $B=0$ measurements (Table II) were used for all subsequent fits. The effective mass value $m^*/m_0=0.35$ used for InAs is substantially higher than the known bulk value ($m^*/m_0=0.24$). This may reflect hot electron effects. We also note that the $k=0$ LO-phonon resonance is shifted to higher frequencies in doped semiconductors and metals due to screening. The high-frequency peaks observed in spectra recorded with the 12 fs system shift with doping as predicted for plasma-LO phonon coupling. We conclude that THz emission from GaAs and InAs at $B=0$ in n-type samples is dominated by plasma oscillations of the extrinsic carriers.

In GaAs, our simulation gives good quantitative agreement with experimental measurements of the integrated power (Fig. 2) and the emission spectrum [Figs. 1(b), 3(a)] for all magnetic fields measured. Within this model, the field dependence of the power can be understood qualitatively as arising from two effects. The first is geometrical: the curvature of the electron trajectories changes the component of the dipole moment perpendicular to outgoing THz beam. Since the sign of the change depends on the field direction, and because there is a perpendicular component even at $B=0$ in our geometry, the minimum intensity does not occur at zero field. At high fields ($\omega_c \gg \gamma$), the electron trajectories are more nearly circular, so that geometrical effects become less important. In this regime, changes in the power reflect the field dependence of the emission spectrum.

The bulk model also describes the field dependence of $E(\omega)$. The model predicts emission at the upper and lower magnetoplasma frequencies, but high frequency emission is suppressed due to the finite excitation time. Therefore, the emission should be dominated by the lower frequency mode, so that the peak of the emission should move to lower frequency with increasing field, as observed. In contrast, a model which ignored plasma oscillations would predict that the peak frequency would follow the cyclotron frequency, and *increase* with field. Under certain conditions, we can expect to resolve the upper and lower frequency modes in our measurements. While the dipole moment of the upper and lower mode have the same sign for very small fields, the contribution from one will change sign as the field is increased, with the lower (upper) mode changing sign at greater positive (negative) fields. This sign change is ob-

served experimentally as a phase shift of π radians in the signal between $B=+0.5-1.0$ T. When the dominant low-frequency mode is suppressed near this sign change, the experimental data clearly show both modes. We conclude that THz emission from n-GaAs in a magnetic field is dominated by bulk magnetoplasma oscillations of the extrinsic carriers.

The dramatic magnetic field dependence of the THz power and emission spectrum of InAs is shown in Figs. 1, 4, and 5 for fields parallel to the sample surface. While the zero-field spectra can be fit by our bulk plasma model, that model fails to predict the low frequency feature observed near 0.35 THz in all of our InAs samples. A three-component plasma model including the photogenerated electrons and light and heavy holes also fails to describe this feature.

However, for this B-field direction, the 2D plasma model predicts emission which peaks at low frequencies due to purely damped carrier motion parallel to the surface. The exact shape of the emission spectrum is determined by the surface damping rate, the electron effective mass and the intersubband plasma frequency. We used a surface damping rate $\gamma_s=2\times10^{12}$ s^{-1} and intersubband frequency $\nu_{12}=12$ THz and fit the THz emission from InAs as a sum of surface and bulk contributions. The parameters of the bulk plasma were determined from measurements at $B=0$. The calculated THz emission spectra are included in Fig. 4(a) and the model qualitatively fits the emission spectra in the range $-0.5\leqslant B\leqslant 0.5$ T in all samples. The model also predicts that the low-frequency component contribution should change sign at $B=0$, while the high-frequency bulklike component should change sign at a finite positive magnetic field. Both of these predictions are in agreement with the data, and we also see two peaks in the spectra recorded at $B=0.1-0.3$ T.

For a B field at 45° to the surface, we have cyclotron motion in the surface layer, and the center of the low-frequency peak should shift to higher frequency with increasing field. The experimental data show a corresponding decrease in the spectral weight at low frequencies (Fig. 6).

The 2D plasma model does not fully describe our data for $|B|>1$ T. In particular, the model predicts that the intensity of the surface mode contribution should increase continuously with increasing field within the measurement range. This increase reflects increased coupling of the initial excitation into the $\omega_-=0$ mode. Experimentally this is not observed (see Fig. 5). However, while the emission amplitudes do not match our model, the peak emission frequencies do follow the predicted magnetoplasma resonance frequencies, so we believe that model is fundamentally sound. The discrepancy may reflect oversimplifications of the model, which assumes that the only effect of the magnetic field is to change the cyclotron frequency. We have not considered any magnetic-field dependence to the initial amplitude of excitation of the surface and bulk modes, or to the damping parameters. We also have not considered coupling between surface and bulk modes. We have used our model to simulate the THz emission from a modulation-doped parabolic quantum well measured by Some and Nurmikko.[10] Here also our model qualitatively reproduces their experimental results, but does not match the measured emission amplitudes. In particular, the model does not predict the peak in the emission power which they observe when the cyclotron and intersubband plasma frequencies cross.

Some of these questions can be answered by additional experimental work. We suggest that THz emission experiments with a midinfrared femtosecond pump tuned to the InAs band gap would allow us to exclude hot-carrier effects and study the process of initial excitation in detail. Further THz emission experiments on modulation-doped quantum wells in magnetic field would also be of interest. Such examinations of a well-characterized quantum well systems would provide an independent test of the surface emission model proposed here. Finally, such work should allow us to optimize the THz generation process in a properly designed modulation-doped heterostructure.

IV. SUMMARY

In summary, we report measurements of photoinduced THz emission from InAs and GaAs as a function of magnetic field. We measured a maximum THz power of 1.6×10^{-13} J/pulse (12 μW average power) from n-InAs (1.8×10^{16} cm^{-3}) at room temperature. The emission process can be described using a semiclassical model of magnetoplasma oscillations of bulk free carriers and damped motion of free carriers in a 2D electron gas. These models provide a simple physical picture of the emission mechanism, but do not fully explain our results. The bulk model describes THz emission from n-GaAs at all magnetic fields, and InAs at $B=0$. A model including both bulk plasma oscillations and THz emission from a surface accumulation layer describes THz emission from InAs in a moderate magnetic field, but this model also fails at fields $|B|>1.0$ T.

ACKNOWLEDGMENTS

This work was supported by the National Science Foundation through the NSF-RUI program (Grant No. DMR-0074622) and the University of Minnesota MRSEC (Grant No. DMR 98-09364). K.U. and T.M. acknowledge support from the Austrian Science Foundation (F016), and J.H. would like to acknowledge partial support from a type-G grant of the Petroleum Research Corporation.

*Electronic address: heyman@macalester.edu

[1] S. L. Chuang, Phys. Rev. Lett. **68**, 102 (1992).

[2] D. H. Auston, K. P. Cheung, and P. R. Smith, Appl. Phys. Lett. **45**, 284 (1984).

[3] C. Fattinger and D. Grischkowsky, Appl. Phys. Lett. **53**, 1480 (1988).

[4] X.-C. Zhang, B. B. Hu, J. T. Darrow, and D. H. Auston, Appl. Phys. Lett. **56**, 1011 (1990).

[5] X.-C. Zhang, Y. Jin, L. E. Kingsley, and M. Weiner, Appl. Phys. Lett. **62**, 2477 (1993).

[6] N. Sarukura, H. Ohtake, S. Izumida, and Z. Liu, J. Appl. Phys. **84**, 654 (1998).

[7] R. McLaughlin, A. Corchia, M. B. Johnston, Q. Chen, C. M. Ciesla, D. D. Arnone, G. A. C. Jones, E. H. Linfield, A. G. Davis, and M. Pepper, Appl. Phys. Lett. **76**, 2038 (2000).
[8] H. Ohtake, S. Ono, M. Sakai, Z. Liu, and T. Tsukamoto, Appl. Phys. Lett. **76**, 1398 (2000).
[9] C. Weiss, R. Wallenstein, and R. Beigang, Appl. Phys. Lett. **77**, 4160 (2000).
[10] D. Some and A. V. Nurmikko, Phys. Rev. B **50**, 5783 (1994).
[11] Q. Wu and X.-C. Zhang, Appl. Phys. Lett. **67**, 3523 (1995).
[12] R. Kersting, J. N. Heyman, G. Strasser, and K. Unterrainer, Phys. Rev. B **58**, 4553 (1998).
[13] R. Kersting, K. Unterrainer, G. Strasser, H. K. Kauffmann, and E. Gornik, Phys. Rev. Lett. **79**, 3038 (1997).
[14] G. Meinert, L. Banyai, P. Gartner, and H. Haug, Phys. Rev. B **62**, 5003 (2000).
[15] D. C. Tsui, Phys. Rev. B **8**, 2657 (1973).
[16] G. S. Bell, T. S. Jones, and C. F. McConville, Appl. Phys. Lett. **71**, 3688 (1997).